Journal of Mathematical Chemistry 24 (1998) 291–319

The Quadrature Discretization Method (QDM) in comparison with other numerical methods of solution of the Fokker–Planck equation for electron thermalization

Ki Leung [a], Bernie D. Shizgal [a,*] and Heli Chen [b]

[a] *Department of Chemistry, University of British Columbia, Vancouver, British Columbia, Canada V6T 1Z1*

[b] *Department of Mathematics, University of British Columbia, Vancouver, British Columbia, Canada V6T 1Z4*

Received 17 September 1997; revised 21 May 1998

The determination of the relaxation of electrons in atomic gases continues to be an important physical problem. The main interest is the determination of the time scale for the thermalization of electrons in different moderators and the nature of the time-dependent electron energy distribution. The theoretical basis for the study of electron thermalization is the determination of the electron distribution function from a solution of the Lorentz–Fokker–Planck equation. The present paper considers a detailed comparison of different numerical methods of solution of the Lorentz–Fokker–Planck equation for the electron distribution function. The methods include a pseudospectral method referred to as the Quadrature Discretization Method (QDM) which is based on non-standard polynomial basis sets, a finite-difference method, and a Lagrange interpolation method. The Fokker–Planck equation can be transformed to a Schrödinger equation, and methods developed for the solution of either equation apply to the other.

1. Introduction

The study of electron thermalization and transport in both atomic [4,6,12,13, 26,31,32,50,62] and molecular moderators [11,21,28–30,41,47,59,63,66,67] continues to be an active field of study. The subject has important applications to radiation chemistry and physics, discharge devices, ionospheric applications, plasma processing of materials and plasma chemistry. The thermalization of energetic electrons in atomic and/or molecular moderators proceeds owing to collisions between the electrons and the constituents of the moderator assumed to be present in large excess. Electron–electron collisions are assumed not to occur and are not included in the theoretical analysis. A complete treatment would require the inclusion of elastic and inelastic collisions, and chemically reactive processes such as ionization and attachment. The

* Also with the Institute of Applied Mathematics.

main interest is to determine the time dependence of the electron energy distribution function starting from some initial arbitrary distribution function. The time scale for the relaxation process and the nature of the time-dependent nonequilibrium distribution function are of importance. The theoretical approach is based on the Boltzmann equation which for electrons with the small electron to moderator mass ratio can be approximated by a Fokker–Planck equation (FPE). Also, the anisotropy of the electron distribution function is expected to be small and two terms in the expansion of the distribution function in Legendre polynomials is sufficient. A standard procedure for the definition of the electron relaxation time is the time required to reach 10% or 1% of the equilibrium energy. Detailed reviews of the current status of the field were presented by Braglia [3] and by Shizgal et al. [55].

The present paper considers a detailed comparison of several different numerical techniques in the study of electron thermalization in the inert gases at low initial energies of the order of several eV. Inelastic collisions are not included and only electron–atom elastic collisions are required. The initial energy loss by inelastic collisions is extremely fast and it is the much slower energy exchange by elastic collisions that determines the relaxation time. Although these atomic systems are not complicated, there is still considerable improvement to be made with the agreement between calculations and measurements [50]. Also, several interesting phenomena have been predicted theoretically. Two unexpected effects have been reported in the course of these studies. One is the "negative mobility effect" for which the transient electron mobility can be negative for some initial transient predicted first by Braglia and Ferrari [5] and later by Shizgal and McMahon [37], and also confirmed with a Monte-Carlo simulation by Koura [27,28]. The experimental observations of the effect were reported by Warman et al. [61]. Another effect is the "negative differential conductivity effect" which refers to the decrease in the electron drift velocity with increasing electric field strength over a particular field range. It was long recognized as arising from inelastic collisions and, therefore, should only occur in molecular systems. Calculations of the drift velocity of electrons in He–Xe and He–Kr mixtures by Shizgal [52] demonstrated that this negative differential conductivity effect can occur for particular concentrations of these mixtures. The effect was later confirmed by Nagpal and Garscadden [40] unaware of the earlier work. There appears to be no experimental confirmation of this effect to date.

There have been numerous theoretical approaches to the problem of electron relaxation in the inert gases. The basis for most of the theoretical work is the Boltzmann equation with realistic data for the electron–atom momentum transfer cross section. The Boltzmann equation is approximated by a FPE and only two terms in the Legendre expansion of the angular part of the distribution function is sufficient. The earliest treatment was carried out by Mozumder [39] and Tembe and Mozumder [58] who assumed that the electron distribution function remains a local Maxwellian with a time-dependent temperature. They derived expressions for the rate of change of the electron temperature from the Boltzmann equation, but the approach did not involve a solution of the Boltzmann equation. Knierem et al. [25] adapted a moment method

of solution of the Boltzmann equation used previously in the study of ion transport. Because of their choice of Burnett functions as basis functions for the expansion of the distribution function, their solutions did not converge well. Koura [27] developed a Monte-Carlo simulation to determine the electron velocity distribution function during the relaxation. Because of the small mass ratio, the computations are very long. Braglia and co-workers [3] employed a variety of techniques including moment methods, finite-difference schemes and Monte-Carlo simulations to solve the FPE. Shizgal and co-workers [34,36,37,54,60] introduced a numerical scheme referred to as the Quadrature Discretization Method (QDM) for the solution of the FPE.

The QDM was developed by Shizgal [51] for the solution of the integral Boltzmann equation and by Shizgal and Blackmore [1] for the solution of differential equations and in the study of nonequilibrium systems with bistable states [2]. It has been used extensively in the study of electron relaxation problems [34,36,60], in the solution of the Schrödinger equation [9,53] and the Navier–Stokes equation [35,64,65]. Details of the application to the Schrödinger equation are presented in the paper immediately following [9]. The QDM is a discretization method based on the evaluation of the solution at a set of quadrature points defined by the roots of the Nth order polynomial of a suitable set orthogonal with respect to some weight function in a specified interval. The main feature of the method is the use of nonclassical polynomials based on a weight function which closely approximates the solution and, hence, provides for rapid convergence. In this sense it differs from the usual spectral methods [7,22] which generally use Fourier series or Chebyshev polynomials. A spectral method refers to the expansion of the solution in a polynomial basis set, whereas a pseudospectral method corresponds to the determination of the solution at a set of points that correspond to the quadrature points associated with the polynomials [7]. These two representations are equivalent and related by a unitary transformation.

There have been several numerical methods proposed for the solution of such Fokker–Planck equations. The most widely used method for the numerical solution of Fokker–Planck equations is a finite-difference method developed some time ago by Chang and Cooper [8], recently refined by Larsen et al. [33] and Epperlein [17]. Robson et al. [48] and Robson and Pritz [49] proposed a derivative matrix technique, based on a Lagrange interpolation, for the solution of differential equations. A very useful discussion of the numerical solution of Fokker–Planck equations was recently published by Park and Petrosian [45].

The present paper is directed towards a detailed comparison of several different numerical methods in comparison with the QDM in the application to electron thermalization in argon. In particular, the QDM is employed with a quadrature based on the steady Davydov distribution function as weight function. The Davydov distribution is characterized by the electron–atom momentum transport cross section and the electric field strength. We construct a polynomial set orthogonal with the Davydov weight function. The numerical technique developed by Gautschi [19] referred to as the Stieltjes procedure is used to generate the orthogonal polynomials and the associated quadrature weights and points. We employ the QDM with this new

quadrature in comparison with the speed polynomials, defined on $[0, \infty]$ with weight function $w(x) = x^2 \exp(-x^2)$ used in most of the previous works. We also consider solutions obtained with a finite-difference technique and the differential quadrature based on the Lagrange interpolation discussed by Robson et al. [48]. These authors suggested that their technique based on a Lagrange interpolation is superior to the QDM.

A comparison of the different discretization schemes is considered in the first instance with regard to the eigenvalue problem defined by

$$L\psi_n(x) = \lambda_n \psi_n(x), \tag{1}$$

where L is the Fokker–Planck operator defined explicitly later, and λ_n and ψ_n are the eigenvalues and eigenfunctions, respectively. We then consider the time evolution of the electron distribution for some initial distribution, with the discretization of the time derivative and advancing the solution in time with either an implict or explicit scheme. The previous work by Shizgal and co-workers [34,36,54,60] considered the time-dependent solution expressed in terms of the eigenfunctions of the Fokker–Planck operator.

An outstanding problem with the eigenfunction technique is that it does not provide a good convergence of the short time dependence if the initial energy is high. This is somewhat expected, since the initial distribution function is generally taken to be a delta function or narrow Gaussian at some energy and the expansion of this initial distribution function in the eigenfunctions of the Fokker–Planck operator is expected to be slow. Also, the evaluation of the eigenfunctions at the initial energy is poor for high initial energies. There have been several attempts to overcome this limitation. Nishigori [42] and Nishigori and Shizgal [43] employed a memory function technique to determine the electron distribution function for small times. Shizgal and Nishigori [56] employed the Wentzel–Kramers–Brillouin approximation in the solution of the eigenvalue problem in order to better approximate the eigenfunctions and improve the small time behaviour. There are other small time approximations discussed by Risken and Voigtlaender [46] and by Susuki [57].

Section 2 of the paper defines the model system considered. The different discretization schemes of the Fokker–Planck operator are outlined in section 3. The time evolution of the solution obtained with several different time discretizations is presented in section 4 for the speed discretizations in section 3.

2. The Lorentz–Fokker–Planck equation: electron thermalization

The motivation for the present study arises from the work of Shizgal and co-workers [3,37,54] on the transient behavior of the distribution function for electrons dilutely dispersed in a large excess of an inert gas at temperature T_b. As mentioned in the introduction, there is a continued interest in the calculation and measurement of the electron relaxation times. Also, these systems provide a useful benchmarking of different numerical methods.

The time-dependent anisotropic spatially uniform electron velocity distribution function is expanded in Legendre polynomials, that is,

$$f(\mathbf{v}, t') = \sum_{l=0}^{\infty} f_l(v, t') P_l(\cos\theta), \tag{2}$$

where θ is the angle between **v** and the polar axis chosen in the direction of the electric field. For the inert gases at low electron energies, for which only elastic collisions need to be included, only the terms in $l = 0$ and $l = 1$ need to be included. With the use of equation (2) one gets the usual two-term approximation [20,24]

$$\frac{\partial f_0}{\partial t'} + \frac{eE}{3m}\left(\frac{\partial}{\partial v} + \frac{2}{v}\right) f_1 = \frac{m}{Mv^2}\frac{\partial}{\partial v}\left[v^3\nu\left(1 + \frac{kT_\mathrm{b}}{mv}\frac{\partial}{\partial v}\right)\right] f_0, \tag{3}$$

$$\frac{\partial f_1}{\partial t'} + \frac{eE}{m}\frac{\partial f_0}{\partial v} = -\nu f_1, \tag{4}$$

where m is the electron mass, M is the moderator mass, E is the electric field strength and the collision frequency $\nu(v) = nv\sigma(v)$, where $\sigma(v)$ is the momentum transfer cross section and n is the number density of the moderator. As discussed in a previous paper [54], we set $\partial f_1/\partial t' = 0$ and substitute f_1 from equation (4) into equation (3). We also define a dimensionless time $t = t'/\tau$, where

$$\frac{1}{\tau} = \frac{nm}{2M}\sigma_0\sqrt{\frac{2kT_\mathrm{b}}{m}} \tag{5}$$

and σ_0 is some convenient hard sphere cross section such that $\widehat{\sigma} = \sigma/\sigma_0$. With the definition of the dimensionless speed variable $x = \sqrt{mv^2/(2kT)}$, we get the equation for f_0 given by

$$\frac{\partial f_0}{\partial t} = \frac{s^2}{x^2}\frac{\partial}{\partial x}\left[2x^4\widehat{\sigma} f_0 + \frac{x^2}{s^2}B(x)\frac{\partial f_0}{\partial x}\right], \tag{6}$$

where

$$B(x) = x\widehat{\sigma}(x) + \frac{(\alpha/s)^2}{x\widehat{\sigma}(x)} \tag{7}$$

and $s = T/T_\mathrm{b}$ is a scaling factor. In equation (7), the quantity α is a field-strength parameter given by

$$\alpha^2 = \frac{M}{6m}\left(\frac{eE}{nkT_\mathrm{b}\sigma_0}\right)^2, \tag{8}$$

In equation (8), the electric field occurs as the density reduced field, E/n, in units of 10^{-17} V cm^2 which is a Townsend (Td). The distribution function is written as

$f_0(x,t) = D(x)g(x,t)$, where $D(x)$ is the equilibrium distribution referred to as the Davydov distribution and given by

$$f_0(x,\infty) = D(x) = C\exp\left[-2s^2\int_0^x \frac{(x')^2\widehat{\sigma}}{B(x')}\,\mathrm{d}x'\right], \tag{9}$$

where C is a normalization constant. The FPE is of the form [37]

$$\frac{\partial g(x,t)}{\partial t} = -Lg(x,t), \tag{10}$$

where

$$L = \frac{1}{s}\left(-A(x)\frac{\partial}{\partial x} + B(x)\frac{\partial^2}{\partial x^2}\right) \tag{11}$$

and

$$A(x) = 2x^2\sigma(x) - \frac{2B(x)}{x} - B'(x). \tag{12}$$

The FPE for this problem can also be rewritten in the usual form

$$\frac{\partial P(x,t)}{\partial t} = \frac{1}{s}\frac{\partial}{\partial x}\left[A(x)P(x,t) + \frac{\partial B(x)P(x,t)}{\partial x}\right] \tag{13}$$

or

$$\frac{\partial P(x,t)}{\partial t} = -\frac{\partial J}{\partial x}, \tag{14}$$

where $J(x,t) = -(A(x)P(x,t) + \partial B(x)P(x,t)/(s\partial x))$ is the flux and vanishes for $P_0(x) = x^2D(x)$. If we set $P(x,t) = D(x)g(x,t)$, then the FPE is of the form

$$\frac{\partial g(x,t)}{\partial t} = \frac{1}{sx^2D(x)}\frac{\partial}{\partial x}\left[x^2D(x)B(x)\frac{\partial g(x,t)}{\partial x}\right]. \tag{15}$$

The method of solution employed in the previous works [3,37,54] involved the formal solution of equation (10) for $g(x,t)$ as given by

$$g(x,t) = \mathrm{e}^{-Lt}g(x,0). \tag{16}$$

If the initial distribution $g(x,0)$ is expanded in the eigenfunctions of L, that is,

$$g(x,0) = \sum_{n=0}^{\infty} a_n\psi_n(x), \tag{17}$$

then the time evolution is given by

$$g(x,t) = \sum_{n=0}^{\infty} a_n\psi_n(x)\mathrm{e}^{-\lambda_n t}, \tag{18}$$

where

$$L\psi_n(x) = \lambda_n\psi_n(x) \tag{19}$$

and the a_n coefficients are determined from the intial condition. The average transport properties can be evaluated and, for example, the electron energy relative to the thermal energy at equilibrium is given by

$$\frac{E(t)}{E_{\text{th}}} = \sum_{n=0}^{\infty} b_n \mathrm{e}^{-\lambda_n t}. \tag{20}$$

If the independent variable, x, is transformed to new variable, y,

$$y = \int_0^x \frac{1}{\sqrt{B(x')}}\,\mathrm{d}x', \tag{21}$$

and we define $\phi_n(y)$ by

$$\phi_n(y) = \sqrt{x^2 D\big(x(y)\big)}\,\psi_n\big(x(y)\big), \tag{22}$$

then the Fokker–Planck eigenvalue equation (equation (19)) is transformed into a Schrödinger equation

$$-\frac{\mathrm{d}^2\phi_n(y)}{\mathrm{d}y^2} + V(y)\phi_n(y) = \lambda_n\phi_n(y). \tag{23}$$

The potential function in the Schrödinger equation is derived from the drift and diffusion coefficients in the Fokker–Planck equation. If $x^2 D(x) = \exp(-\int W(y)\,\mathrm{d}y)$, then $V(y)$ is given by

$$V(y) = \frac{1}{4}W^2 - \frac{1}{2}\frac{\mathrm{d}W}{\mathrm{d}y}, \tag{24}$$

where

$$W(y) = \frac{A(x(y))}{\sqrt{B(x(y))}} + \frac{\mathrm{d}B/\mathrm{d}y}{2B(x(y))}. \tag{25}$$

The potential functions obtained in this way belong to the class of potentials that occur in supersymmetric quantum mechanics [10,14]. Examples of such potential functions were shown in a previous paper [54]. We could consider the determination of the eigenvalues with the solution of the Schrödinger equation (equation (23)), as done by Shizgal and Chen [53] and in the paper immediately following [9]. However, the accuracy we consider in this paper is far greater than can be obtained with the transformation to the Schrödinger equation because of a loss of accuracy in the numerical integration of equation (21).

3. Numerical solution of the Fokker–Planck eigenvalue problem

3.1. The Quadrature Discretization Method (QDM)

The solution of differential equations by differential quadrature methods is based on the representation of the derivative operator, $\mathrm{d}/\mathrm{d}x$, in a discrete basis. The distribu-

tion function is solved at a set of points which are the quadrature points, that is, the roots of the Nth order polynomial of the set orthogonal with respect to some weight function, $w(x)$. The method has been discussed at length in previous papers [2,37,53,54]. In this section, we present a brief outline of the QDM.

Consider a set of polynomials $R_n(x)$, orthogonal with respect to the weight function $w(x)$ on the interval $[a, b]$, that is,

$$\int_a^b w(x)R_n(x)R_m(x)\,\mathrm{d}x = \delta_{nm}. \tag{26}$$

The numerical integration of some function $f(x)$ with weight function $w(x)$ is given by

$$\int_a^b w(x)f(x)\,\mathrm{d}x \approx \sum_{i=1}^{N} w_i f(x_i), \tag{27}$$

where w_i and x_i are the weights and points of the quadrature, respectively. The points are the roots of the Nth order polynomial, i.e., $R_N(x_i) = 0$. The discrete representation of a function $f(x)$ is the values of $f(x)$ at the discrete points, that is, $f(x_i) = \widetilde{f}(x_i)/\sqrt{w_i}$. The factor $\sqrt{w_i}$ symmetrizes the transformations discussed below. The representation of $f(x)$ is given by the expansion coefficients, a_n, of $f(x)$ in the basis set $\{R_n(x)\}$. There is a unitary (or orthogonal) transformation between the discrete representation and the representation in the polynomial basis, that is,

$$\widetilde{f}(x_i) = \sum_{n=0}^{N-1} \sqrt{w_i}R_n(x_i)a_n, \tag{28}$$

$$a_n = \sum_{j=1}^{N} \sqrt{w_j}R_n(x_j)\widetilde{f}(x_j). \tag{29}$$

The matrix elements of the symmetric transformation are given by

$$T_{in} = \sqrt{w_i}R_n(x_i). \tag{30}$$

If in equation (28) x_i is replaced with x and equation (29) is used for a_n, then one obtains an Nth order interpolation for $f(x)$ given by

$$f(x) = \sum_{j=1}^{N} I_j^{(N)}(x)f(x_j), \tag{31}$$

where the interpolation function, $I_j^{(N)}(x)$, is given by

$$I_j^{(N)}(x) = w_j \sum_{n=0}^{N} R_n(x)R_n(x_j). \tag{32}$$

The algorithm for differentiation in the discrete basis is given by differentiating equation (31) and using equation (32), and one has for $\widetilde{f}(x_i)$ that

$$\frac{\mathrm{d}\widetilde{f}(x_i)}{\mathrm{d}x} = \sum_{j=1}^{N} D_{ij}\widetilde{f}(x_j), \tag{33}$$

where the derivative operator in equation (33), $D_{ij} = \sqrt{w_i/w_j}(\mathrm{d}I_j^{(N)}(x)/\mathrm{d}x)|_{x=x_i}$, is given by

$$D_{ij} = \sqrt{w_i w_j}\sum_{n} R_n'(x_i)R_n(x_j). \tag{34}$$

The algorithms (equations (33) and (34)) can be used to reduce a general differential operator equation to a set of coupled algebraic equations in the function evaluated at the quadrature points. One important aspect of this discretization procedure is to preserve the self-adjoint property of the Fokker–Planck operator, that is, the discretized representation of the Fokker–Planck operator should be symmetric. Another important consideration is the choice of mesh points (or, equivalently, basis functions) determined by the quadrature weight function, $w(x)$.

A useful choice of weight function is the equilibrium distribution $P_0(x)$, for which we have the basis set $\{Q_n(x)\}$ defined by

$$Q_n(x) = \left[\frac{w(x)}{P_0(x)}\right]^{1/2} R_n(x), \tag{35}$$

which satisfies the orthogonality relation

$$\int_0^\infty P_0(x)Q_n(x)Q_m(x)\,\mathrm{d}x = \delta_{nm}. \tag{36}$$

The matrix elements of the operator L in this basis set are given by

$$L_{nm} = \int_0^\infty P_0(x)Q_n(x)LQ_m(x)\,\mathrm{d}x, \tag{37}$$

which with an integration by parts becomes

$$L_{nm} = -\int_0^\infty P_0(x)B(x)Q_n'(x)Q_m'(x)\,\mathrm{d}x, \tag{38}$$

where the integrated term determines the boundary conditions which corresponds to zero flux at both boundaries, so that

$$x^2D(x)B(x)\frac{\partial g(x,t)}{\partial x}\bigg|_{x=0} = x^2D(x)B(x)\frac{\partial g(x,t)}{\partial x}\bigg|_{x=\infty} = 0. \tag{39}$$

In terms of the polynomials $\{R_n(x)\}$ (equation (35)), and weight function $w(x)$ we have with equation (38)

$$L_{nm} = -\int_0^\infty B(x)w(x)\left[\frac{\mathrm{d}}{\mathrm{d}x} + h(x)\right]R_n(x)\left[\frac{\mathrm{d}}{\mathrm{d}x} + h(x)\right]R_m(x), \tag{40}$$

where

$$h(x) = \frac{w'(x)}{2w(x)} - \frac{[x^2D(x)]'}{2x^2D(x)}. \tag{41}$$

If we now use the quadrature rule for the weight $w(x)$, we have that

$$L_{nm} = -\sum_{k=1}^{N} B(x_k)w_k\left[R'_m(x_k) + h(x_k)R_m(x_k)\right]\left[R'_n(x_k) + h(x_k)R_n(x_k)\right]. \tag{42}$$

If the derivatives are evaluated with the QDM algorithm (equation (33)), we have that

$$\begin{aligned} L_{mn} = &-\sum_{j=1}^{N}\sqrt{w_j}R_m(x_j)\sum_{i=1}^{N}\sqrt{w_i}R_n(x_i) \\ &\times\sum_{k=1}^{N}B(x_k)\left[D_{ki} + h(x_k)\delta_{ik}\right]\left[D_{kj} + h(x_k)\delta_{jk}\right]. \end{aligned} \tag{43}$$

With the transformation between the representation in a basis set and the discrete representation of the function, we have the QDM representative in the discrete basis given by

$$L_{ij} = -\sum_{k=1}^{N} B(x_k)[D_{ik} + h_i\delta_{ik}][D_{jk} + h_j\delta_{jk}]. \tag{44}$$

Further details of the derivations in this section have appeared in previous papers [1,2,53,54].

3.2. Lagrange interpolation (LI)

In a recent paper, Robson et al. [48] suggested that the use of a Lagrange interpolation algorithm with a uniform grid in place of an interpolation based on a set of orthogonal polynomials would be more efficient. Their result, previously obtained by other workers [18], based on the Lagrange interpolation polynomial, is given by

$$l_i(x) = \frac{\prod_{j=1}^{N-1}(x - x_j)}{\prod_{j\neq i=1}^{N-1}(x_i - x_j)}, \tag{45}$$

for which $l_i(x_j) = \delta_{ij}$, also satisfied by $I_i^{(N)}(x_j)$ of equation (32). The points can be chosen anywhere on the interval of interest as the roots of the polynomial

$$P_N(x) = k_N \prod_{j=1}^{N-1} (x - x_j), \tag{46}$$

where k_N is the coefficient of x^N. It, therefore, follows that

$$l_i(x) = \frac{P_N(x)}{(x - x_i)P'_N(x_i)}, \tag{47}$$

and the derivative matrix is

$$D_{ij} = l'_i(x_j). \tag{48}$$

We use the form of the Fokker–Planck operator given by equation (15) and write the representation of the Fokker–Planck operator in the form

$$L_{ij} = \frac{[(x_i^2 B(x_i)D(x_i))' D_{ij} + x_i^2 B(x_i)D(x_i)]D_{ij}^{(2)}}{x_i^2 D(x_i)}, \tag{49}$$

which is not symmetric as is the QDM representation (equation (44)). Robson et al. [48] suggested that this is preferred, since the evaluation of the derivative matrix is faster with equations (47) and (48) rather than with equation (34), and the free choice of the grid points is advantageous. They evaluated the accuracy of the QDM and Lagrange differentiation algorithms by considering the calculation of the second derivative of some arbitrary function. In a subsequent paper, Robson and Pritz [49] applied their approach to the solution of several other problems.

3.3. Finite-difference (FD) scheme

The self-adjoint form of the Fokker–Planck equation (equation (15)) was shown to be consistent with zero flux at the boundaries (equation (39)). This boundary condition is also related to particle conservation

$$\frac{\partial}{\partial t} \int_0^\infty D(x)g(x,t)x^2 \,\mathrm{d}x = x^2 D(x)B(x)\frac{\partial g(x,t)}{\partial x}\bigg|_{x=\infty}^{\infty} = 0. \tag{50}$$

Any useful discretization would have to ensure particle conservation which yields $\lambda_0 = 0$. We discretize the speed variable according to $0 = x_1 < x_2 < x_3 < \cdots < x_N = x_{\max}$ with $x_{i+1} = x_i + \Delta x$ and $\Delta x = x_{\max}/(N-1)$, where $x_{\max}$ is the speed point chosen large enough, so that the flux boundary condition is satisfied. We also introduce a shifted grid at the midpoint defined by $x_{i+1/2} = x_i + \Delta x/2$. With a centered difference for the derivative

$$\frac{\partial g(x,t)}{\partial x}\bigg|_{x_{i+1/2}} \approx \frac{g(x_{i+1},t) - g(x_i,t)}{\Delta x}, \tag{51}$$

the finite-difference representation of the eigenvalue problem is

$$\sum_{j=1}^{N} L_{ij}\phi_n(x_i) = \lambda_n \phi_n(x), \tag{52}$$

where

$$L_{ii} = \frac{1}{(\Delta x)^2}\frac{x_i^2 D_i B_i + x_{i+1}^2 D_{i+1} B_{i+1}}{x_{i+1/2}^2 D_{i+1/2}}, \quad i = 1, \ldots, N, \tag{53}$$

$$L_{i,i-1} = -\frac{1}{(\Delta x)^2}\frac{x_i^2 D_i B_i^2}{x_{i+1/2}^2 D_{i+1/2}}, \qquad i = 2, \ldots, N, \tag{54}$$

$$L_{i,i+1} = -\frac{1}{(\Delta x)^2}\frac{x_{i+1}^2 D_{i+1} B_{i+1}}{x_{i+1/2}^2 D_{i+1/2}}, \qquad i = 1, \ldots, N-1, \tag{55}$$

with the understanding that the first term in the fraction on the RHS of equation (53) vanishes for $i = 1$ and the second term vanishes for $i = N$ in order to enforce the boundary conditions.

4. Time-dependent solutions of the Fokker–Planck equation

The previous work on the thermalization of electrons employed the eigenfunction expansion solution of the FPE. One of the difficulties with this approach is that the calculation converges poorly for very small times and large initial energies for an initial delta function distribution. The reason for this is that the expansion coefficients in equation (17) require the calculation of the eigenfunctions at large argument and these are not accurately calculated. This aspect of the eigenfunction expansion was discussed at length in previous papers. In this section we use a time discretization in place of the eigenfunction expansion.

4.1. Finite-difference time discretization

Following Larsen et al. [33], we discretize the velocity variable as described earlier in section 3. We set $t = n\Delta t$ for the discrete time variable and use a backward Euler difference for the time derivative, that is,

$$\frac{\partial g(x,t)}{\partial t} = \frac{g_i^{n+1} - g_i^n}{\Delta t}, \tag{56}$$

where $g_i^n = g(x_{i+1/2}, n\Delta t)$. The FD version for the time-dependent FPE (equation (15)) becomes

$$\frac{\partial g(x,t)}{\partial t} = \frac{g_i^{n+1} - g_i^n}{\Delta t}$$

$$= \frac{x_{i+1}^2 D_{i+1} B_{i+1}(g_{i+1}^{n+1} - g_i^{n+1}) - x_i^2 D_i B_i g_i^{n+1} - g_{i-1}^{n+1}}{(\Delta x)^2 x_{i+1/2}^2 D_{i+1/2}}, \tag{57}$$

which after rearranging terms can be written as

$$\sum_{j=1}^{N} V_{ij} g_j^{n+1} = g_i^n, \tag{58}$$

where V is a tridiagonal matrix whose elements are given by

$$V_{ii} = 1 + \Delta t L_{ii}, \quad i = 1, \ldots, N, \tag{59}$$

$$V_{i,i-1} = \Delta t L_{i,i-1}, \quad i = 2, \ldots, N, \tag{60}$$

$$V_{i,i+1} = \Delta t L_{i,i+1}, \quad i = 1, \ldots, N-1. \tag{61}$$

The new values of the distribution g_i^{n+1}, $i = 1, \ldots, N$, are then obtained from equation (59) by inverting V. Notice that the matrix V is diagonally dominant, i.e., $|V_{ii}| > |V_{i,i-1}| + |V_{i,i+1}|$, and that the off-digonal elements are negative; therefore, if $g_i^n > 0$ for all i, then $g_i^{n+1} > 0$ for all i, and the positivity of the distribution is preserved in time as mentioned by Larsen et al.

The choice of a backward Euler difference for the time derivative leading to an implicit scheme is dictated by stability arguments. For an explicit scheme, it can be easily seen that the matrix elements are not uniformly bounded functions of x near $x = 0$ when an electric field is present ($\alpha \neq 0$). We also observed that, for an explicit scheme, the zero eigenvalue is inaccurate and, hence, an explicit scheme would lead to unphysical behaviour and the relaxation to equilibrium is not guaranteed.

4.2. QDM and Lagrange interpolation

The discretized version of equation (10) becomes

$$\frac{g_i^{n+1} - g_i^n}{\Delta t} = L_{ij} g_j^{n+1}, \tag{62}$$

where L_{ij} is the matrix representation of the Fokker–Planck operator, given by either equation (44) or equation (49). This results in the following implicit scheme for the time evolution of the distribution function given by

$$g_j^{n+1} = \sum_{i=1}^{N} [\delta_{ij} - \Delta t L_{ij}]^{-1} g_i^n. \tag{63}$$

The discretized form of L_{ij} for the two cases are as given previously.

5. Calculations and results

We consider the relaxation of electrons in argon for which there are several published electron–argon momentum transfer cross sections. Since this paper is directed

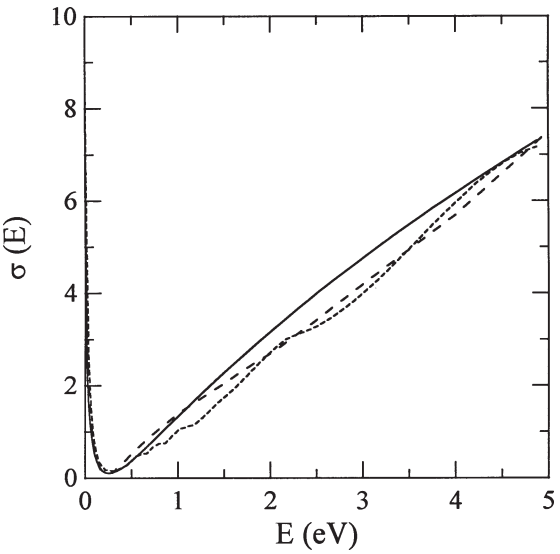

Figure 1. Energy variation fo the momentum transfer cross section for electron–argon collisions. Solid curve is the fit given by equation (64). The dashed and dotted curves are the cross sections reported by Haddad and O'Malley [23] and Mozumder [39], respectively.

towards a comparison of numerical methods, we chose to fit the actual cross section to a simple analytic form given by

$$\sigma(E) = \big(7.8945 - 3.0397\sqrt{E} + 30.7265E\big)\big/\big(1 + 5.1640\sqrt{E}\,\big), \tag{64}$$

where E is in eV and $\sigma(E)$ is in $\times 10^{-16}$ cm^2. The previous works [34,36,37,54] generally employed the actual tabulated cross sections and a cubic spline interpolation. In this paper, we use the simple analytic model to avoid introducing additional errors in the spline fitting of the cross section, however small they are in practice. Figure 1 shows the energy dependence of this cross section given by equation (64) (solid curve) in comparison to the cross section by Mozumder [39] (dotted curve) and by Haddad and O'Malley [23] (dashed curve). The fit to the Ramsauer–Townsend minimum is particularly accurate. We have chosen to study Ar, because the electron-Ar cross section has this strong energy dependence.

With the cross section specified, the FPE is well defined. The convergence of the eigenvalues of the Fokker–Planck operator for the three different discretizations, FD, LI and QDM, with speed points is shown in table 1 for zero applied electric field. In this case, the Davydov distribution reduces to a Maxwellian and the "speed points" that are used are defined by the weight function $w(x) = x^2 \exp(-x^2)$ [51]. For the FD method and the LI, the semi-infinite range has to be cut off at some $x_{\max}$ as indicated in the footnote to the table. The QDM has an additional flexibility in terms of the scaling parameter, s, which can be increased or decreased to spread the points over a wider range or to create a denser grid near the origin. The value of s listed in the table optimizes the rate of convergence. As can

Table 1
Comparison of the convergence of eigenvalues with FD, LI, and QDM approaches for electrons in argon.[a]

N	λ_1	λ_2	λ_3	λ_5	λ_7
			FD[b]		
10	4.2065018	6.0252130	7.7433925	14.926823	30.951015
20	3.7779542	5.9687808	8.7864926	15.983947	23.109246
30	3.7135707	5.9512106	8.8741400	16.789326	26.454696
50	3.6823834	5.9423225	8.9142694	17.157737	27.716141
70	3.6740821	5.9399242	8.9247708	17.254000	28.044467
100	3.6697460	5.9386723	8.9302677	17.304654	28.219512
120	3.6684861	5.9383105	8.9318775	17.319588	28.271937
			LI[c]		
20	3.6192863	6.2197787	8.7710260	19.265133	43.300454
30	3.6680821	5.9435491	8.8431719	15.314643	28.361252
40	3.6656115	5.9368816	8.9387666	17.259492	25.748304
50	3.6656267	5.9373678	8.9346936	17.347228	28.326278
60	3.6656280	5.9373511	8.9346356	17.338753	28.283583
70	3.6656258	5.9372353	8.9348420	17.343482	28.271660
100	3.6656279	5.9373500	8.9346399	17.338821	28.276115
			QDM (speed)[d]		
10	6.1840221	13.3297100			
20	3.6934786	6.0043920	9.1035057	18.866842	38.168512
30	3.6656545	5.9374256	8.9349024	17.347670	28.303877
32	3.6656352	5.9373816	8.9347739	17.338882	28.304116
35	3.6656288	5.9373529	8.9346425	17.339099	28.279519
38	3.6656282	5.9373510	8.9346407	17.338853	28.275974
40	3.6656281	5.9373510	8.9346395	17.338803	28.276495
42		5.9373509	8.9346395	17.338806	28.276138
45			8.9346393	17.338802	28.276163
50					28.276131
60					28.276129

[a] $E/n = 0.0$ Td, λ_n in units of $\tau^{-1} = (nm/(2M))\sigma_0\sqrt{2kT_b/m}$.
[b] FD with $x_{max} = 4.8$.
[c] LI with Legendre grids and $x_{max} = 8.0$.
[d] Speed with scale factor, $s^2 = 0.31$.

be seen from the results in the table, the convergence of the λ_n with the QDM is superior to the other methods. It is useful to note that the results in table 1 to the maximum orders shown are reasonably consistent. For example, for λ_7, the LI with 100 points and the QDM with 60 points differ by only 1 in the 7th significant figure.

With an increase in the electric field, the steady distribution that is the Davydov distribution peaks at higher reduced speed as shown in figure 2. Curve (a) in figure 2 is for $E/n = 0$ and corresponds to a Maxwellian. The other two curves are Davydov distributions at $E/n = 0.25$ and 0.50 Td, respectively. Table 2 shows the convergence

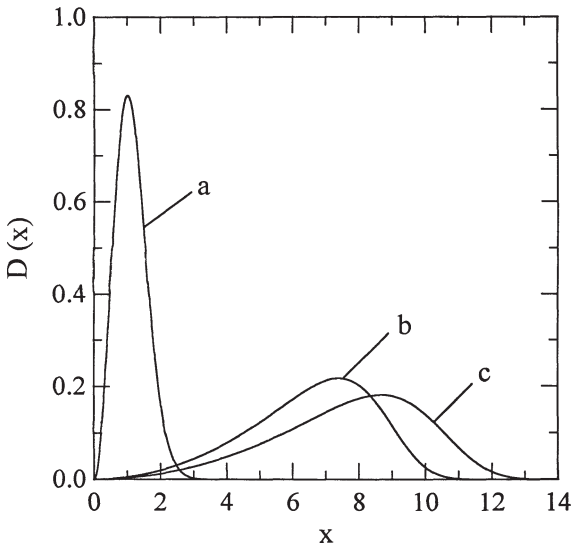

Figure 2. The energy variation of the steady electron Davydov distribution for different electric field strengths with E/n equal to (a) 0, (b) 0.25 and (c) 0.50 Td.

of the eigenvalues with the different discretizations for an electric field strength of $E/n = 0.25$ Td. We show the results with the QDM for both speed points and quadrature points with the Davydov distribution. The FD and LI schemes require much larger values of $x_{\max}$ and the scaling factor for the QDM with speed points is also increased. The results in table 2 for the convergence of the eigenvalues for the four different schemes demonstrates that the QDM based on the Davydov distribution as the weight function provides the fastest convergence. Excellent agreement is obtained for the eigenvalues shown with LI and QDM with speed and Davydov weight functions. This is also demonstrated in table 3 for a still larger electric field, $E/n = 0.50$ Td. The convergence of the eigenvalues is still fastest with the QDM and the Davydov weight function.

Figure 3 shows the variation of $\ln \lambda_n$ versus n for $E/n = 0.25$ Td for different numbers of points: (a) $N = 10$, (b) $N = 20$, (c) $N = 40$ and (d) $N = 60$. Figure 3(A) shows the results for QDM with Davydov points, whereas figure 3(B) is for the FD method. The portions of these curves that coincide for the converged eigenvalues gives an indication of the actual variation of λ_n versus n. At some value of n for a given N, the curves depart rather quickly from this converged λ_n versus n variation. Figure 3 shows $\ln \lambda_n$, so that the higher order eigenvalues, which are not converged, are very large. Notice that, with the FD method, the results given by curves (a)–(c) do not coincide for lower values of n. A more detailed comparison of the results with the FD and the QDM is shown in figure 4 for $N = 40$ and $N = 60$. The QDM provides accurate results for small n, but the nonconverged eigenvalues are much larger than the eigenvalues obtained with the FD method.

Table 2
Comparison of the convergence of eigenvalues with FD, LI, and QDM approaches for electrons in argon.[a]

N	λ_1	λ_2	λ_3	λ_5	λ_9
			FD[b]		
10	.33941476(3)	.74461440(3)	.14108440(4)	.54032190(4)	
30	.34231218(3)	.86931571(3)	.14919656(4)	.28941745(4)	.56952524(4)
50	.34235202(3)	.87004783(3)	.14966735(4)	.29389261(4)	.62575032(4)
70	.34235623(3)	.87011773(3)	.14971979(4)	.29444701(4)	.63287130(4)
100	.34235733(3)	.87013221(3)	.14973401(4)	.29461716(4)	.63581345(4)
			LI[c]		
15	.34173489(3)	.86293925(3)	.14551342(4)	.30569352(4)	.67165473(4)
20	.34236128(3)	.87010035(3)	.14970006(4)	.29462674(4)	.54615085(4)
22	.34235818(3)	.87011456(3)	.14971715(4)	.29421504(4)	.51149006(4)
25	.34235748(3)	.87012965(3)	.14973782(4)	.29463182(4)	.63175395(4)
28	.34235767(3)	.87013188(3)	.14973904(4)	.29470714(4)	.63121553(4)
30		.87013172(3)	.14973885(4)	.29469742(4)	.63553764(4)
35				.29469732(4)	.63575199(4)
40				.29469729(4)	.63573630(4)
50					.63573638(4)
			QDM (speed)[d]		
20	.34289609(3)	.87143973(3)	.15394656(4)	.46817396(4)	
25	.34236587(3)	.87030912(3)	.14977423(4)	.30528649(4)	
30	.34235769(3)	.87013265(3)	.14974718(4)	.29507212(4)	.73053706(4)
35	.34235767(3)	.87013179(3)	.14973895(4)	.29474139(4)	.65021538(4)
38		.87013172(3)	.14973887(4)	.29470361(4)	.63971760(4)
40		.87013171(3)	.14973885(4)	.29469863(4)	.63953852(4)
50				.29469729(4)	.63577734(4)
60				.29469729(4)	.63573643(4)
70					.63573638(4)
			QDM (Davydov)		
5	.34427329(3)	.89684722(3)			
8	.34235742(3)	.87016409(3)	.15103419(4)		
10	.34235770(3)	.87014349(3)	.14975221(4)	.34716352(4)	.79385157(5)
12	.34235768(3)	.87013369(3)	.14974456(4)	.29813215(4)	.45048506(5)
15	.34235768(3)	.87013174(3)	.14973894(4)	.29491739(4)	.14263194(5)
18	.34235767(3)	.87013172(3)	.14973886(4)	.29470191(4)	.65877825(4)
20			.14973885(4)	.29469777(4)	.64560309(4)
25				.29469729(4)	.63582864(4)
30				.29469729(4)	.63573676(4)
35					.63573638(4)

[a] $E/n = 0.25$ Td, τ_n in units of $\tau^{-1} = (nm/(2M))\sigma_0\sqrt{2kT_b/m}$.
[b] FD with $x_{max} = 13.6$.
[c] LI with Legendre grids and $x_{max} = 13.7$.
[d] Speed with scale factor, $s^2 = 2.65$.

Table 3
Comparison of the convergence of eigenvalues with FD, LI, and QDM approaches for electrons in argon.[a]

N	λ_1	λ_2	λ_3	λ_5	λ_9
			FD[b]		
10	.53872902(3)	.11995596(4)	.21483903(4)		
20	.54347279(3)	.13659116(4)	.23212179(4)	.42746820(4)	
30	.54379648(3)	.13711155(4)	.23515801(4)	.45764519(4)	.91334196(4)
40	.54385693(3)	.13719719(4)	.23567357(4)	.46251932(4)	.97707943(4)
50	.54387599(3)	.13722003(4)	.23581409(4)	.46390824(4)	.99455015(4)
70	.54388811(3)	.13723136(4)	.23588534(4)	.46465072(4)	.10047569(5)
80	.54389045(3)	.13723291(4)	.23589549(4)	.46476416(4)	.10067101(5)
100	.54389289(3)	.13723416(4)	.23590381(4)	.46486298(4)	.10089314(5)
			LI[c]		
20	.54391212(3)	.13724848(4)	.23600394(4)	.47224649(4)	
22	.54389133(3)	.13722978(4)	.23587963(4)	.46161520(4)	
25	.54389617(3)	.13723542(4)	.23591640(4)	.46538858(4)	
28	.54389650(3)	.13723486(4)	.23590899(4)	.46493478(4)	.10535303(5)
30	.54389641(3)	.13723483(4)	.23590903(4)	.46494517(4)	.10077973(5)
35			.23590902(4)	.46494433(4)	.10084415(5)
40				.46494430(4)	.10083041(5)
45					.10083027(5)
50					.10083026(5)
			QDM (speed)[d]		
20	.56951180(3)	.16108781(4)	.33917322(4)		
25	.54402094(3)	.13729568(4)	.23661662(4)	.55979996(4)	.34590212(5)
30	.54389772(3)	.13723712(4)	.23591362(4)	.46947691(4)	.14922917(5)
35	.54389641(3)	.13723487(4)	.23590995(4)	.46505376(4)	.10727918(5)
40		.13723483(4)	.23590902(4)	.46494732(4)	.10146367(5)
50				.46494431(4)	.10083266(5)
60				.46494430(4)	.10083026(5)
70					.10083026(5)
			QDM (Davydov)		
5	.54572180(3)	.13954983(4)			
8	.54389718(3)	.13724642(4)	.23795336(4)		
10	.54389639(3)	.13723495(4)	.23593244(4)	.51559993(4)	
12	.54389642(3)	.13723488(4)	.23591053(4)	.46958088(4)	
15		.13723483(4)	.23590913(4)	.46512740(4)	.26604484(5)
18			.23590902(4)	.46494607(4)	.10272763(5)
20				.46494450(4)	.10175485(5)
25				.46494430(4)	.10083568(5)
30					.10083027(5)
35					.10083026(5)

[a] $E/n = 0.50$ Td, λ_n in units of $\tau^{-1} = (nm/(2M))\sigma_0\sqrt{2kT_b/m}$.
[b] FD with $x_{max} = 16.1$.
[c] LI with Legendre grids and $x_{max} = 17.0$.
[d] Speed with scale factor, $s^2 = 3.1$.

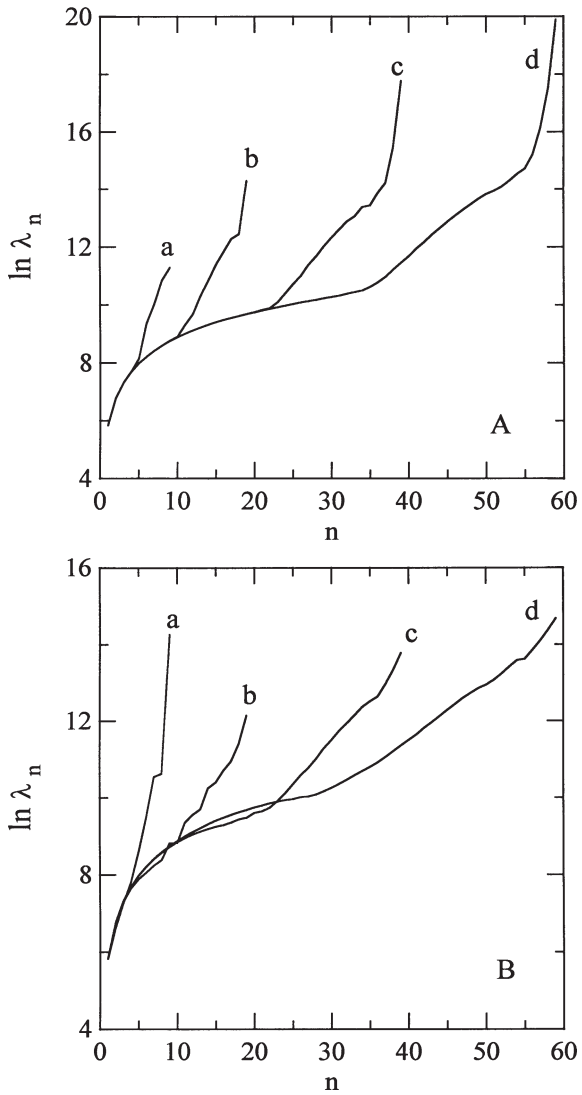

Figure 3. Variation of the eigenvalues versus the index n with the (A) QDM and (B) FD method. The number of grid points, N, is equal to (a) 10, (b) 20, (c) 40 and (d) 60.

Figure 5 shows a comparison of the variation of the error, $\Delta E_n^{(N)}$, given by

$$\Delta E_n^{(N)} = \left| E_n^{(N)} - E_n^{\text{exact}} \right|, \tag{65}$$

in the calculated values of the eigenvalues λ_2 and λ_5 versus the number of quadrature or grid points. The "exact" result is taken to be the results with the QDM and 70 Davydov points. For the QDM (figure 5(A)), the error decreases rapidly with increasing N and the semi-logarithmic plot is nearly-linear. The convergence is nearly exponential with increasing N and "spectral" accuracy is said to be satisfied [7,18,22].

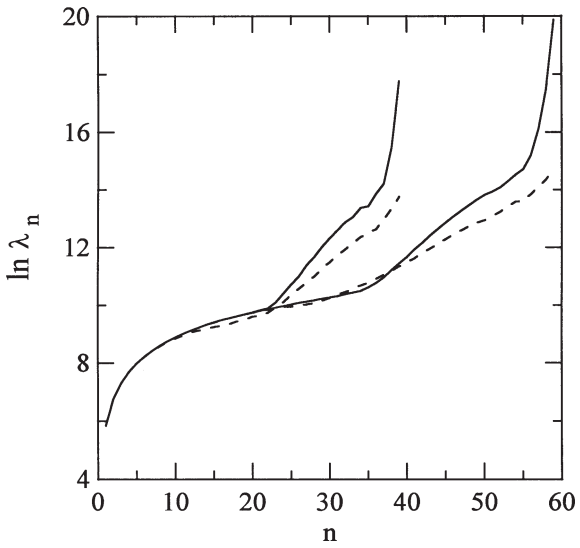

Figure 4. Same as figure 3 with the solid curves the QDM results and the dashed curves the FD results, with N equal to 40 and 60.

By contrast, the decrease in the error for the FD method is much slower. One surprising result is the oscillations in the curves in figure 5(A). If a variational theorem holds in this application, the eigenvalues for a particular N should be an upper bound for the actual eigenvalue and the convergence should be monotonic from above.

We also show the convergence of two eigenfunctions at the intermediate field studied, $E/n = 0.25$ Td. Figures 6 and 7 show the convergence of the eigenfunctions $\psi_3(x)$ and $\psi_7(x)$ versus the number of quadrature points retained. The solid curve is the result using the QDM with the Davydov distribution as weight function and $N = 70$. This is considered to be the converged or exact result against which the lower order solutions are compared. The convergence of the QDM with Davydov points is exceptionally rapid, and very good agreement is obtained with just $N = 8$. The FD results are nonmontonic in that the results for $N = 10$ appear in less agreement with the converged eigenfunctions than for $N = 8$. All the methods give converged eigenfunctions for $N = 30$. The results for ψ_7 shown in figure 7, are comparable, except that the convergence with the FD and LI are quite poor for lower order. These require at least $N = 30$ to give reasonable results. The QDM results show nearly-converged results with $N = 20$.

The time-dependent electron distribution was determined with an initial Gaussian distribution at some initial energy,

$$f_0(x, 0) = Nx^2 \exp\bigl(-\alpha(x - x_0)^2\bigr), \tag{66}$$

where $\alpha = 4$ and $x_0 = 9.5$, and N is a normalization constant. The choice of the parameters is arbitrary. In the previous work, the time dependence was deter-

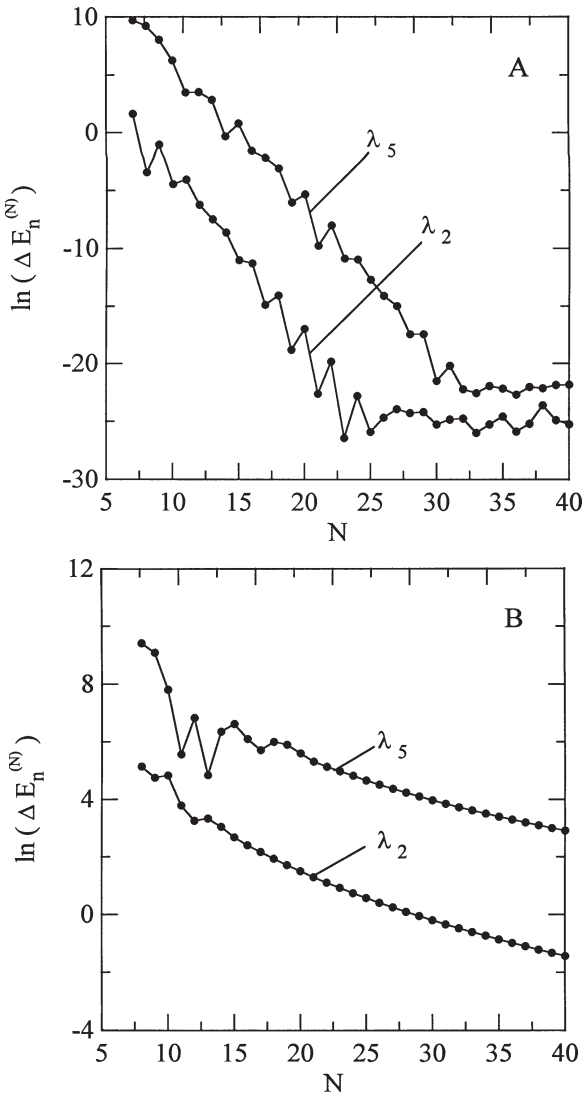

Figure 5. Variation of the error in λ_2 and λ_5 versus the number of grid points, N, with the (A) QDM and (B) FD method.

mined in terms of the expansion in the eigenfunctions (equation (18)). This is a useful method, except that it can give poor results for short times. The reason for this is that the short-time behavior is controlled by the largest eigenvalues which are not converged. Also, the coefficients that fit the distribution function to the initial distribution are evaluated with the eigenfunctions which are not accurately calculated at the highest energies [42,43,56]. Instead of the eigenfunction expansion for the time-dependent solution, we have here employed the FD discretization of the time derivative as described in section 4.1. The condition number [7,18,22] of the ma-

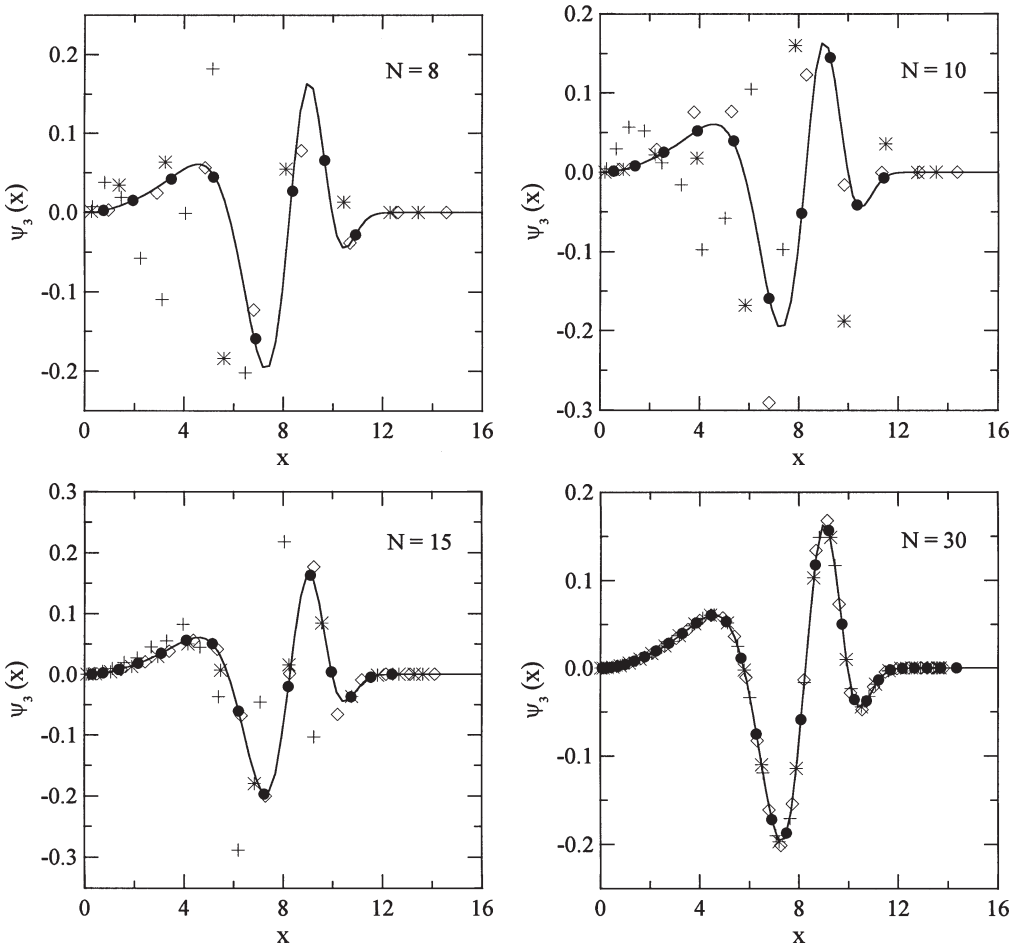

Figure 6. Convergence of the eigenfunction ψ_3 versus the number of grid points, N, for the LI, FD, and QDM techniques.

trix representative of the Fokker–Planck operator is defined by $\lambda_{\max}/\lambda_1$. The condition number for the QDM is larger than for the FD method (figures 3 and 4), and the maximum time step in an explicit time integration would be smaller for the QDM than for the FD method. However, the time integrations in this paper were all carried out with an implicit method. For higher-dimensional problems, an explicit method may have to be used because of the greater computer costs of the implicit method.

The time evolution of the electron distribution function was obtained with the FD scheme with 100 points and is shown in figure 8 at several times for $E/n = 0.25$ Td. The initial distribution is labelled by (a) and the steady Davydov distribution is labelled by (e). The time evolution of the average electron energy calculated with this time-dependent distribution function is shown in figure 9. Although the FD discretization

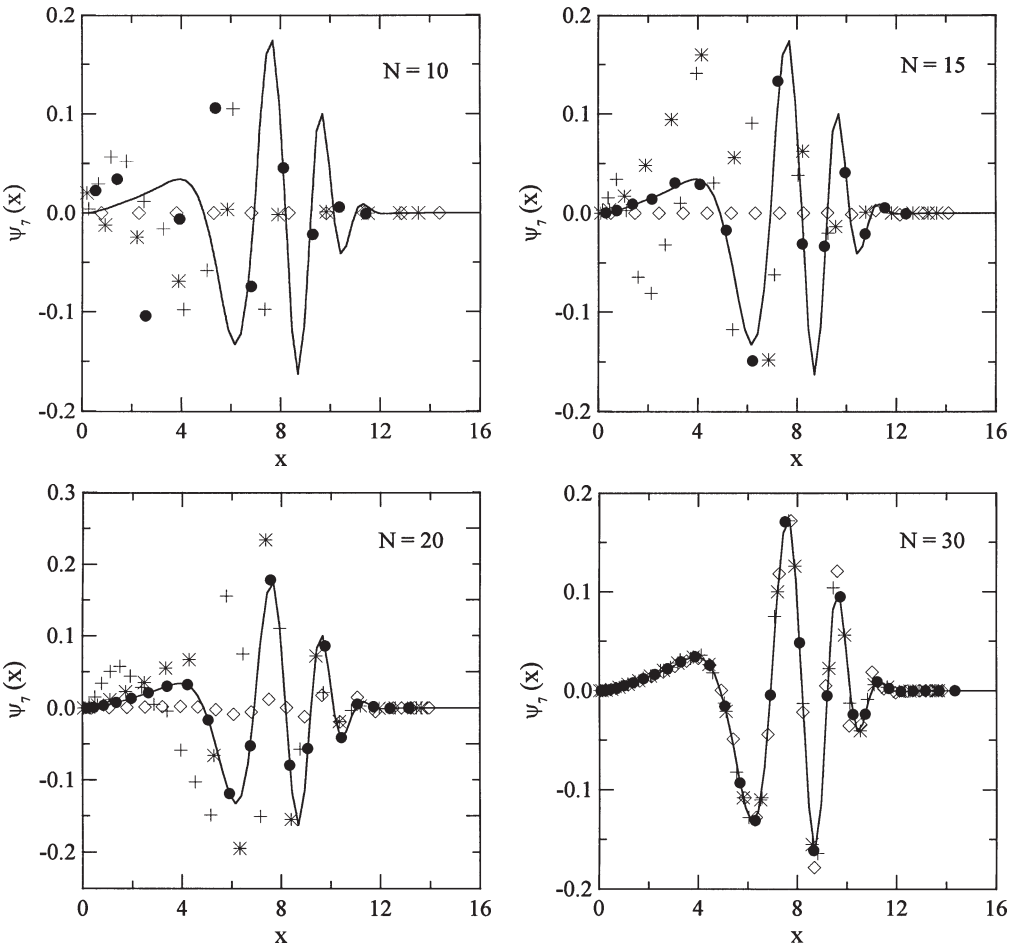

Figure 7. Convergence of the eigenfunction ψ_7 versus the number of grid points, N, for the LI, FD, and QDM techniques.

of the Fokker–Planck operator gives the slowest convergence of the eigenvalues, it provides the most reliable results for the time evolution determined as described in section 4.2. This is because the discretization guarantees positivity of the electron distribution function at all times. The other schemes give oscillations in the distribution function, particularly at small times.

We show the convergence of the distribution function at three different times in figures 10–12. For the very short time, $t = 0.00025$ (figure 10), the results with the LI scheme denoted by the asterisks (*) gives the worst convergence. The results with $N = 10$, 20 and 30 are not converged to the exact result. The QDM results are an improvement but give oscillatory and negative distributions with a small number of points. All three discretizations give accurate results with $N = 30$ in figure 10(D). For the intermediate time, $t = 0.001$ (figure 11), the LI method still gives poor results with

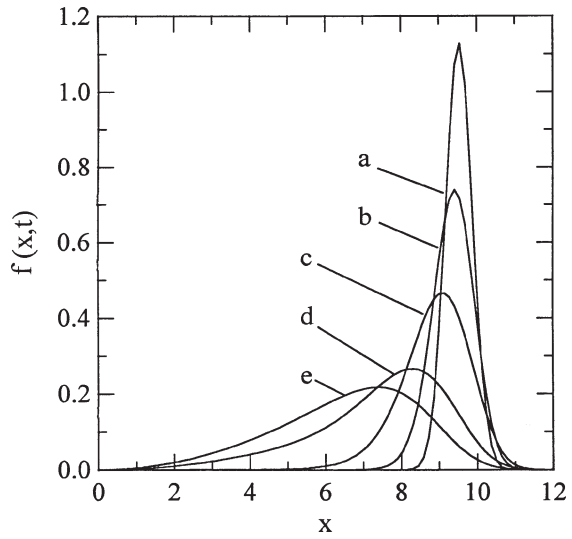

Figure 8. Time variation of the electron distribution function calculated with the FD method and 100 points. The curve labelled (a) is the initial Gaussian distribution and the curve labelled (e) is the steady Davydov distribution. The other curves correspond to reduced times equal to (b) 0.00025, (c) 0.001 and (d) 0.004.

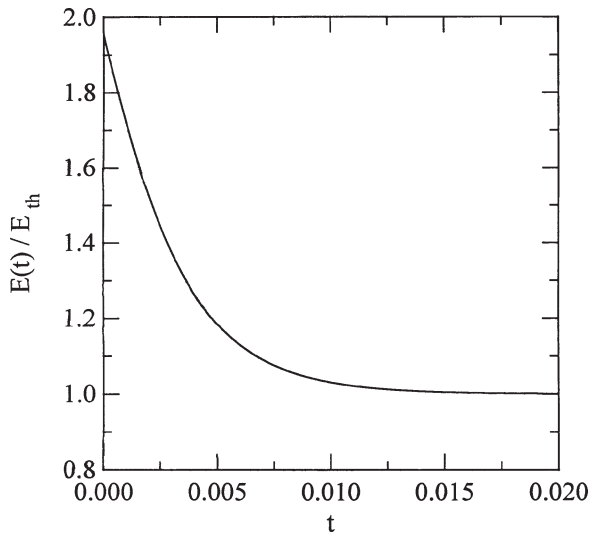

Figure 9. Time variation of the average electron energy.

a small number of points, but there is an improvement in the results with the QDM. In fact, the QDM results appear to be marginally better than the FD near the peak of the distribution. For the longest time, $t = 0.004$ (figure 12), the LI discretization still shows considerable error at low order even with 20 points. All three discretization methods give good agreement with 30 grid points.

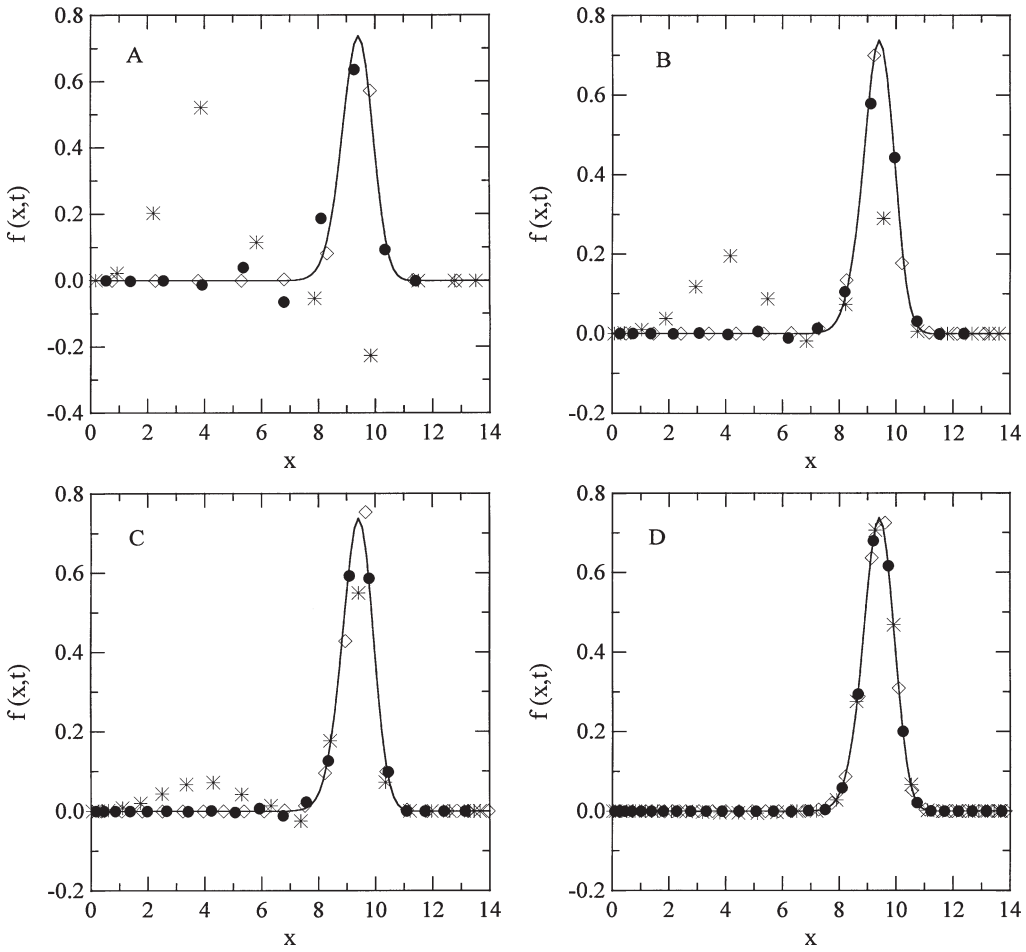

Figure 10. Convergence of the electron distribution at short times, $t = 0.00025$, with the different discretizations. The solid line is the result with the FD method and 100 points. The results with the LI, FD and QDM are denoted by asterisks, diamonds and solid symbols, respectively. The number of grid points, N, is equal to (A) 10, (B) 15, (C) 20 and (D) 30.

6. Summary

In this paper, we have considered a comparison of several numerical methods for the solution of the Lorentz–Fokker–Planck equation for the thermalization of electrons in argon. We have compared (1) the Quadrature Discretization Method (QDM) with quadrature points based on speed polynomials orthogonal with respect to the weight function $w(x) = x^2 \mathrm{e}^{-x^2}$; (2) the QDM with quadrature points based on nonclassical polynomials orthogonal with respect to the Davydov distribution; (3) a discretization based on the Lagrange interpolation formula; and (4) a finite-difference scheme. The convergence of the eigenvalues with the quadrature points based on the Davydov dis-

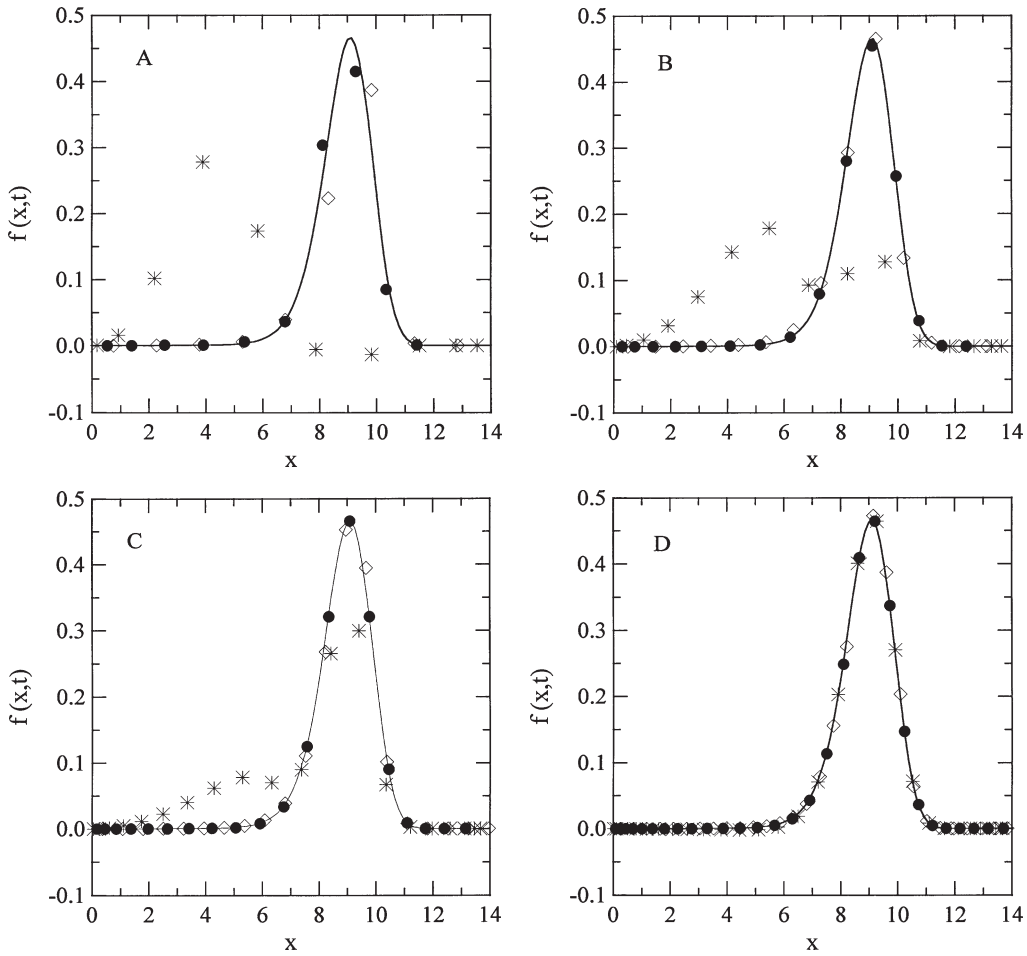

Figure 11. Convergence of the electron distribution at moderate times, $t = 0.001$; see caption for figure 10.

tribution as weight function was superior to the other methods. The time evolution of the electron distribution function was evaluated with an implicit time integration for all four discretization schemes. The finite-difference scheme provided the best results for a given number of grid points. The reason for this is that the algorithm used preserved the positivity of the distribution function. The Lagrange interpolation provided the worst results. The QDM provided results intermediate between the finite-difference method and the Lagrange interpolation. Further work is in progress to develop an algorithm based on the QDM that will preserve positivity of the distribution function. We will also consider a preconditioner [7,18,22] for the QDM matrix representative of the Fokker–Planck operator so as to reduce the condition number of the matrix.

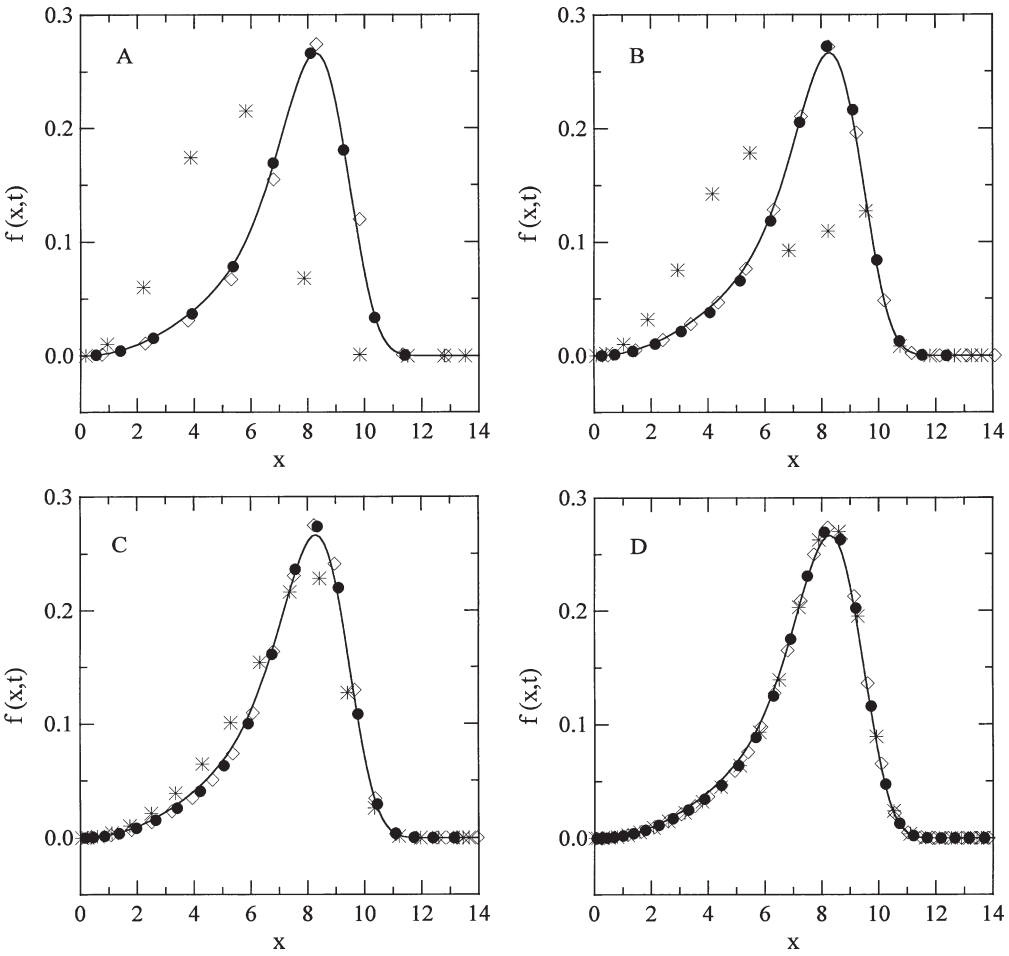

Figure 12. Convergence of the electron distribution at moderate times, $t = 0.004$; see caption for figure 10.

Acknowledgements

This research was supported by a grant from the Natural Sciences and Engineering Research Council of Canada. We are grateful to Dr. Lucio Demeio for computer programs related to the finite-differencing of the Fokker–Planck equation.

References

[1] R. Blackmore and B. Shizgal, J. Comput. Phys. 55 (1984) 313.
[2] R. Blackmore and B. Shizgal, Phys. Rev. A 31 (1985) 1855.
[3] G.L. Braglia, Riv. Nuovo Cimento 18 (1995) 1.
[4] G.L. Braglia, M. Diligenti, J. Wilhelm and R. Winkler, Nuovo Cimento D 12 (1990) 257.
[5] G.L. Braglia and L. Ferrari, Nuovo Cimento B 4 (1971) 245.

[6] G.L. Braglia and P. Minari, Contr. Plasma Phys. 34 (1994) 711.
[7] C. Canuto, M.Y. Hussaini, A. Quarteroni and T.A. Zang, *Spectral Methods in Fluid Dynamics* (Springer, New York, 1987).
[8] J.S. Chang and G. Cooper, J. Comput. Phys. 6 (1970) 1.
[9] H. Chen and B.D. Shizgal, J. Math. Chem. 24 (1998) 321.
[10] A. Comtet, A.D. Bandrauk and D.K. Campbell, Phys. Lett. 150B (1985) 159.
[11] H. Date, S. Yachi, K. Kondo and H. Tagashira, J. Phys. D 25 (1992) 42.
[12] M. Dillon and M. Kimura, Phys. Rev. A 52 (1995) 1178.
[13] P.J. Drallos and J.M. Wadehra, Phys. Rev. A 40 (1989) 1967.
[14] R. Dutt, A. Khare and U.P. Sukhatme, Am. J. Phys. 56 (1988) 163.
[15] M.J. Englefield, J. Stat. Phys. 52 (1988) 369.
[16] M.J. Englefield, Physica A 167 (1990) 877.
[17] E.M. Epperlein, Laser Particle Beams 12 (1994) 257; J. Comput. Phys. 112 (1994) 291.
[18] B. Fornberg, *A Practical Guide to Pseudospectral Methods* (Cambridge University Press, Cambridge, 1996).
[19] W. Gautschi, J. Comput. Appl. Math. 12 (1985) 61.
[20] A. Gilardini, *Low Energy Electron Collisions in Gases* (Wiley, New York, 1974).
[21] N. Goto and T. Makabe, J. Phys. D 23 (1990) 686.
[22] D. Gottlieb and S. Orszag, *Numerical Analysis of Spectral Methods* (SIAM-CBMS, Philadelphia, 1977).
[23] G.N. Haddad and T.F. O'Malley, Austr. J. Phys. 35 (1982) 35.
[24] L.G.H. Huxley and R.W. Crompton, *The Diffusion and Drift of Electrons in Gases* (Wiley, New York, 1974).
[25] K.D. Knierim, M. Waldman and E.A. Mason, J. Chem. Phys. 77 (1982) 943.
[26] K. Kondo and H. Tagashira, J. Phys. D 26 (1993) 1948.
[27] K. Koura, J. Chem. Phys. 84 (1986) 6227; 82 (1985) 2556; 81 (1984) 4180.
[28] K. Koura, J. Chem. Phys. 87 (1987) 6481.
[29] K. Kowari, Phys. Rev. A 53 (1996) 853.
[30] K. Kowari, L. Demeio and B.D. Shizgal, J. Chem. Phys. 97 (1992) 2061.
[31] I. Krajcar-Bronic and M. Kimura, J. Chem. Phys. 103 (1995) 7104.
[32] I. Krajcar-Bronic, M. Kimura and M. Inokuti, J. Chem. Phys. 102 (1996) 6552.
[33] E.W. Larsen, C.D. Livermore, G.C. Pomraning and J.G. Sanderson, J. Comput. Phys. 61 (1985) 359.
[34] K. Leung, J.C. Barrett and B. Shizgal, Chem. Phys. 147 (1990) 257.
[35] G. Mansell, W. Merryfield, B. Shizgal and U. Weinert, Comput. Methods Appl. Mech. Engrg. 104 (1993) 295.
[36] D.R.A. McMahon, K. Ness and B. Shizgal, J. Phys. B 19 (1986) 2759.
[37] D.R.A. McMahon and B. Shizgal, Phys. Rev. A 31 (1985) 1894.
[38] T. Miyazawa, Phys. Rev. A 39 (1989) 1447.
[39] A. Mozumder, J. Chem. Phys. 72 (1980) 1657, 6289; 74 (1981) 6911; 76 (1982) 3277.
[40] R. Nagpal and A. Carscadden, Phys. Rev. Lett. 73 (1994) 1598.
[41] K.F. Ness and R. Robson, Phys. Rev. A 34 (1986) 2185.
[42] T. Nishigori, Nucl. Sci. Engrg. 108 (1991) 347; Chem. Phys. Lett. 221 (1994) 492.
[43] T. Nishigori and B. Shizgal, J. Chem. Phys. 89 (1988) 3275.
[44] H. Okamoto, J. Phys. A 23 (1990) 5535.
[45] B.T. Park and V. Petrosian, Astrophys. J. Suppl. Ser. 103 (1996) 255; Astrophys. J. 446 (1995) 699.
[46] H. Risken and K. Voigtlaender, Z. Phys. B 54 (1984) 253.
[47] R. Robson and K.F. Ness, Phys. Rev. A 33 (1986) 2068.
[48] R.E. Robson, K.F. Ness, G.E. Sneddon and L.A. Viehland, J. Comput. Phys. 92 (1991) 213.
[49] R.E. Robson and A. Pritz, Austr. J. Phys. 46 (1993) 465.

[50] H. Shimamori and T. Sunagawa, Chem. Phys. Lett. 267 (1997) 334.
[51] B. Shizgal, J. Comput. Phys. 41 (1981) 309.
[52] B. Shizgal, Chem. Phys. 147 (1990) 271.
[53] B.D. Shizgal and H. Chen, J. Chem. Phys. 104 (1996) 4137.
[54] B. Shizgal and D.R.A. McMahon, Phys. Rev. A 32 (1985) 3669.
[55] B. Shizgal, D.A.R. McMahon and L.A. Viehland, Radiat. Phys. Chem. 34 (1989) 35.
[56] B. Shizgal and T. Nishigori, Chem. Phys. Lett. 171 (1990) 493.
[57] M. Suzuki, in: *Order and Fluctuations in Equilibrium and Nonequilibrium Statistical Mechanics*, eds. G. Nicolis, G. Dewel and J.W. Tuerner (Wiley, New York, 1981).
[58] B.L. Tembe and A. Mozumder, J. Chem. Phys. 78 (1983) 2030; 81 (1984) 2492; Phys. Rev. 27 (1983) 3274.
[59] S. Ushiroda, S. Kajita and Y. Kondo, J. Phys. D 23 (1990) 47.
[60] L.A. Viehland, S. Ranganathan and B. Shizgal, J. Chem. Phys. 88 (1988) 362.
[61] J.M. Warman, U. Sowada and M.P. de Haas, Phys. Rev. A 31 (1985) 1974.
[62] R. Winkler, J. Wilhelm, G.L. Braglia and M. Diligenti, Nuovo Cimento D 12 (1990) 975.
[63] S. Yachi, H. Date, K. Kitamori and H. Tagashira, J. Phys. D 24 (1991) 573.
[64] H.H. Yang, B.R. Seymour and B.D. Shizgal, Comp. Fluids 23 (1994) 829.
[65] H.H. Yang and B. Shizgal, Comput. Methods Appl. Mech. Engrg. 118 (1994) 47.
[66] M. Yousfi, A. Hennad and A. Alkan, Phys. Rev. E 49 (1994) 3264.
[67] M. Yumoto, Y. Kuroda and T. Sakai, J. Phys. D 24 (1991) 1594.